Article

Twisted Push-Pull Probes with Turn-On Sulfide Donors

VEROLET, Quentin, *et al*.

Abstract

Planarizable and polarizable dithieno[3,2-b;2′,3′-d]thiophene (DTT) dimers have been introduced recently as fluorescent probes that report on membrane fluidity with red shifts in excitation, i.e. planarization in the ground state. In this study, we elaborate on the hypothesis that twisted push-pull probes could perform best in the presence of one unorthodox substituent that acts as a weak acceptor with electron-rich and as a strong donor with electron-poor aromatics. According to Hammett constants, we thought that sulfides could provide access to such a conceptually innovative donor-acceptor switch. To elaborate on this hypothesis, we here describe the design, synthesis and evaluation of a comprehensive series of twisted push-pull probes with turn-on sulfide donors. Their planarization is explored in lipid bilayer membranes of different thickness and fluidity from liquid-disordered to liquid-ordered and solid-ordered phases. Results from membranes are compared to the planarization of turn-on mechanophores in crystals, proteins, and cyclodextrin macrocycles of varied diameter.

Reference

VEROLET, Quentin, *et al*. Twisted Push-Pull Probes with Turn-On Sulfide Donors. *Helvetica chimica acta*, 2017, vol. 100, no. 2, p. e1600328

DOI : 10.1002/hlca.201600328

Twisted Push-Pull Probes with Turn-On Sulfide Donors

Quentin Verolet, Marta Dal Molin, Adai Colom, Aurélien Roux, Laure Guénée, Naomi Sakai, and Stefan Matile*

School of Chemistry and Biochemistry, National Centre of Competence in Research (NCCR) Chemical Biology, University of Geneva, Geneva, Switzerland,
Phone: +41 22 379 6523, E-mail: stefan.matile@unige.ch

Planarizable and polarizable dithieno[3,2-b;2′,3′-d]thiophene (DTT) dimers have been introduced recently as fluorescent probes that report on membrane fluidity with red shifts in excitation, i.e. planarization in the ground state. In this study, we elaborate on the hypothesis that twisted push-pull probes could perform best in the presence of one unorthodox substituent that acts as a weak acceptor with electron-rich and as a strong donor with electron-poor aromatics. According to Hammett constants, we thought that sulfides could provide access to such a conceptually innovative donor-acceptor switch. To elaborate on this hypothesis, we here describe the design, synthesis and evaluation of a comprehensive series of twisted push-pull probes with turn-on sulfide donors. Their planarization is explored in lipid bilayer membranes of different thickness and fluidity from liquid-disordered to liquid-ordered and solid-ordered phases. Results from membranes are compared to the planarization of turn-on mechanophores in crystals, proteins and cyclodextrin macrocycles of varied diameter.

Keywords: Fluorescent Probes • Mechanophores • Push-Pull Systems • Deplanarization • Membranes • Macrocycles • Proteins

Introduction

The color change of lobsters, crabs or shrimps during cooking originates from a combined deplanarization and depolarization of the astaxanthin chromophore in response to the thermal denaturation of the surrounding β-barrel protein.[1][2] Most important biological processes such as vision, particularly color vision, operate similarly.[3] The application of this more complex lesson from nature to fluorescent probes has received little attention so far. However, this combination of planarization and polarization in the ground state appeared most intriguing, particularly with regard to fluorescent probes that could report on key characteristics of biomembranes[4-8] such as fluidity,[5] potential[6][7] as well as the so far elusive membrane tension.[8]

The concept of planarizable[9] push-pull[10] probes has been introduced in 2012 with mechanophore **1** (*Figs. 1, 2*).[11] This original probe **1** and its optimized congener **2**[12] consist of an oligothiophene[13] with methoxy donors and cyanovinyl acceptors (*Fig. 2*). Methyl groups are installed along the scaffold to twist the oligomer out of conjugation. The origin of this deplanarization is the repulsion between the methyls and the σ hole on the proximal sulfur atoms,[14] a situation that can be referred to as chalcogen bond repulsion, or chalcogen anti-bonds (*Fig. 1*, ★). This deplanarization of twisted push-pull probes **1** or **2** occurs in a fluid medium, such as solvents or liquid disordered (L_d) lipid bilayer membranes. In the confining environment of solid-ordered (S_o) membrane, however, the probe is planarized. This planarization results in a better conjugation, better communication between donor and acceptor, and thus a red shift of the excitation maximum by $\Delta\lambda_{ex}$ = +44 nm from λ_{ex} = 416 nm to λ_{ex} = 460 nm with the best probe **2**.

The introduction of the concept of "fluorescent flippers" marked the next milestone in the design of planarizable push-pull probes.[15] The term was coined to describe monomers in oligomeric probes that

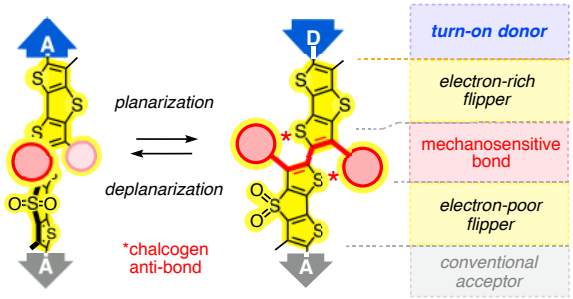

Figure 1. The concept of twisted push-pull probes with turn-on donors. In the twisted resting state in solution, they are "turned off" to support blue-shifting deplanarization and prevent oxidation of the decoupled electron-rich flipper. Upon planarization of the mechanophore in confined space, they "turn on" to support the planarizing, red-shifting push-pull system.

have a) high fluorescence (to keep emitting when twisted out of conjugation) and b) large surface area (to feel the environment really well).[15] Dithieno[3,2-b;2′,3′-d]thiophenes (DTTs),[16] particularly their most fluorescent S,S-dioxides, were selected as the first fluorescent flippers. Installed in the twisted push-pull probe **3**, the phase change from L_d to S_o membranes shifted excitation maximum from λ_{ex} = 453 nm to a broad maximum at λ_{ex} = 498 – 533 nm, and increased fluorescence lifetimes from 2.2 to 4.3 ns (compatible with fluorescence-lifetime imaging microscopy: FLIM[4][5]).[15]

Further improvement in the mechanosensitivity could be anticipated by enforcing the push-pull strength. In mechanophore **3**, the electron-rich DTT and the electron-poor DTT S,S-dioxide already provide a push-pull system. The DTT S,S-dioxide acceptor is further supported by a withdrawing aldehyde. However, the donor is missing on the electron-rich DTT in flipper probe **3** because in twisted form, i.e., disconnected from the acceptors, additional donors cause spontaneous oxidative degradation.[17] In twisted form, the electron-rich DTT should ideally be

stabilized by an acceptor that further supports deplanarization and turns into a donor only upon planarization and connection with the acceptor part of the probe.

Supported by early computational studies,[18] Hammett constants σ_p = +0.03 and σ_p^+ = -0.60[19] suggested that ethyl sulfides could serve as turn-on donors in planarizable push-pull probes.[17] This "amphiphilic" nature of sulfur atoms in organic molecules originates from their high polarizability, their poor electronegativity, and their long bonds. The electron-accepting nature of sulfur atoms accounts, for example, for the high acidity of thiols and thioketals compared to alcohols and ketals, respectively.[20] It presumably involves empty 3d or antibonding σ* orbitals as acceptors, the latter being explicitly supported by the high acidity of equatorial compared to axial protons in thioketals. The long C-S bonds and the diffuse 3p orbitals of the sulfur reduce contributions from π bonds to donate electrons. Thioketones are unstable for this reason.[21] However, the electron-donating nature of sulfur atoms grows in significance in combination with electron poor partners such as carbocations.[18] As substituents in π-acidic aromatic systems such as naphthalenediimides, sulfides donate electrons almost as well as ethers.[22]

Preliminary studies confirmed that "all-sulfur" model flippers **4** with turn-on sulfide donors are stable (*Fig. 2*).[17] Their record Stokes shift of 9300 cm^{-1} in solution suggested that turn-on sulfides indeed act as acceptors in the twisted ground state (causing blue-shifted excitation) and donors in the planar, highly polarized push-pull excited state (causing red-shifted emission). Time-resolved emission spectra revealed the occurrence of planarization from the twisted Franck-Condon state to the planar S1 state in 3.5 ps.[17] Encouraged by these model studies in solution, we decided to prepare a series of twisted push-pull mechanophores with turn-on sulfide donors to study their properties in solid crystals, lipid bilayer membranes of varied fluidity, in proteins and in cyclodextrin macrocycles of varied diameter.

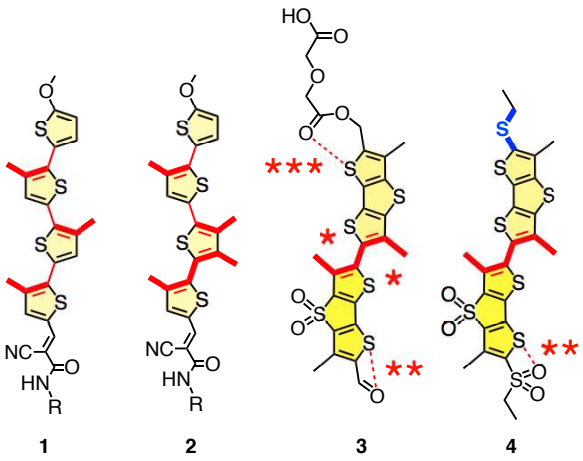

Figure 2. The evolution of planarizable push-pull probes, from the original quaterthiophene **1** to the all-sulfur turn-on flipper model **4**. R: charged groups for delivery to and orientation in membranes. ★: σ-hole repulsion for deplanarization. ★★: Possible 1,4 S-O chalcogen bond to prevent rotational quenching. ★★★: Possible 1,6 (or 1,4) S-O chalcogen-bonding long-distance donor.

Results and Discussion

Design.

One of the unique advantages of all-sulfur turn-on flipper **4** is the possibility to easily build on both push and pull termini of the mechanophore (*Fig. 2*).[7] This was of interest to explore, for example, the importance of the orientation of the push-pull macrodipole in lipid bilayer membranes for sensing applications.[7] Constitutional isomers **5** and **6** have been designed to address this question (*Fig. 3*). Oriented by an anionic anchor, probes **5** and **6** will partition into vesicular membranes with the negative end of their macrodipole pointing toward the interior and the exterior, respectively. In constitutional isomers **7** and **8**, the same question is repeated with a shorter anchor and a more permanent negative charge. The series of mechanosensitive membrane probes with turn-on donors was completed with the replacement of the sulfone acceptors in **5** and **7** by cyano acceptors in **9** and **10** and formyl acceptors in **11** (*Fig. 4*). With formyl and cyano acceptors, macrodipole inversion as in **5**–**8** is obviously not possible. In controls **12** and **13**, cyano acceptors are tested for the original design of flipper **3** and the variation with a shorter, permanently charged anchor.

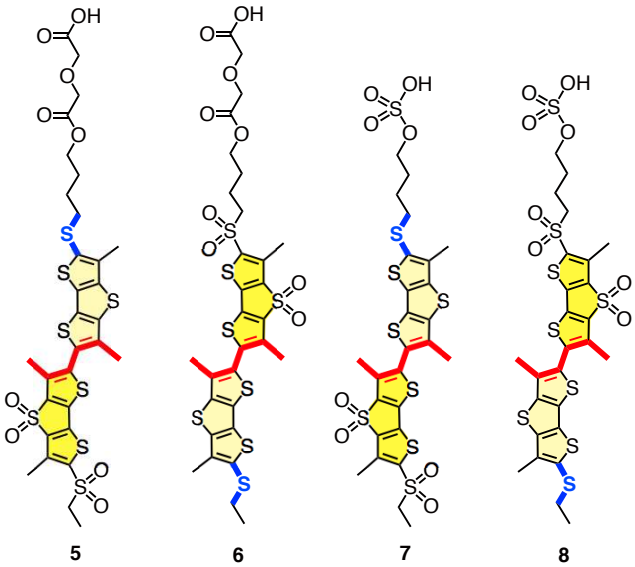

Figure 3. The first generation of twisted push-pull probes with turn-on sulfide donors, focusing on all-sulfur architectures and the orientation of the push-pull dipole.

Synthesis.

The new mechanophores **5**–**13** were accessible in a few steps from commercially available starting materials. The synthesis of probes **5**, **6** and **12** is outlined in *Scheme 1*. Details on the synthesis of all probes can be found in the Supplementary Material (*Schemes S1–S4*, *Figs. S13–S58*).[23]

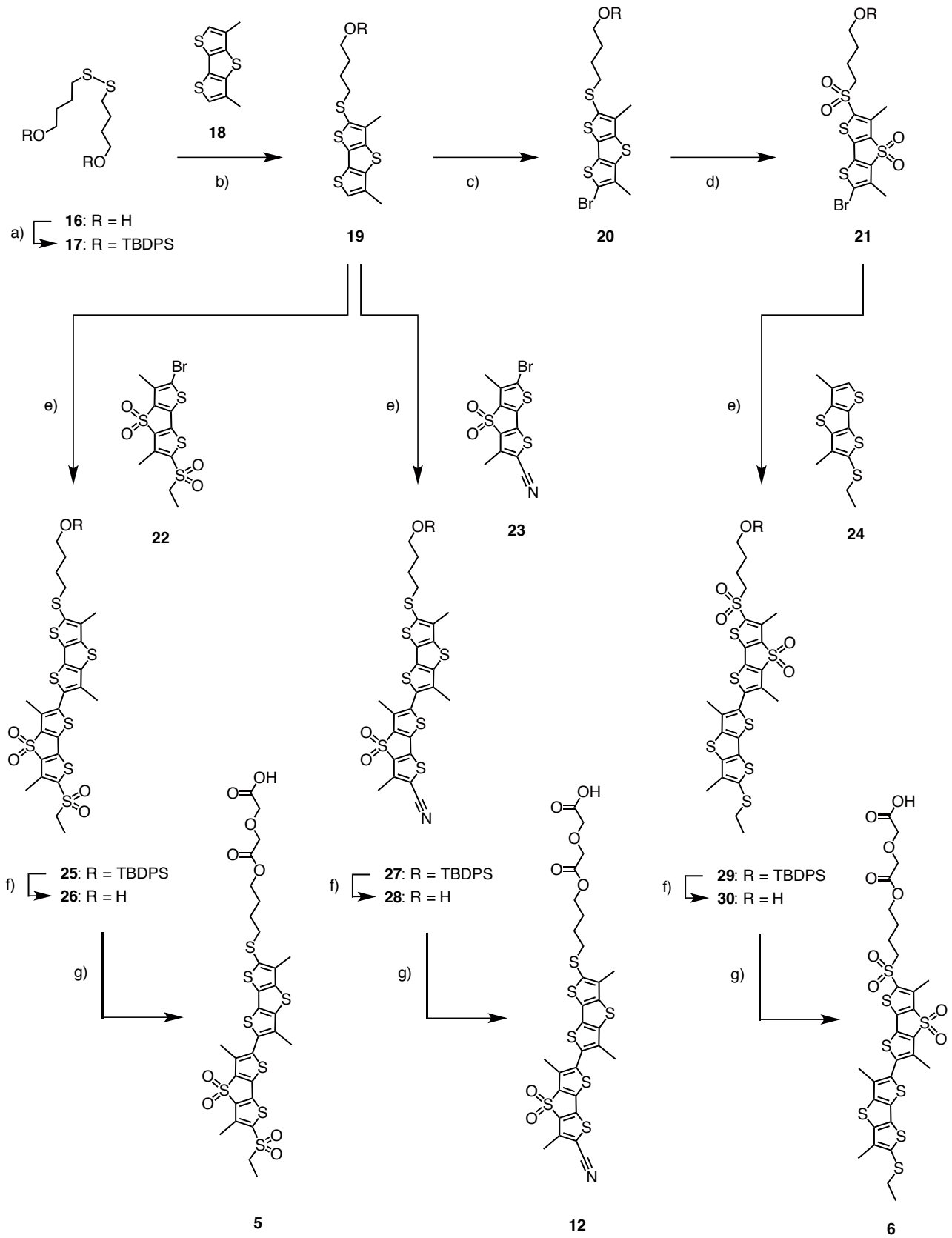

Scheme 1. a) Imidazole, TBDPSCl, THF, rt, 12 h, 92%; b) LDA, **18**, THF, -78 °C to rt, 24 h, 26%; c) NBS, DCM, rt, 3 h, 88%; d) mCPBA, $CHCl_3$, rt, 4 h, 53%; e) 1. LDA, $SnCl(Bu)_3$, THF, -78 °C to rt, 1 h, 2. $Pd(PPh_3)_4$, DMF, 70 °C, 24 h, 20% (**25**), 31% (**27**), 60% (**29**); f) TBAF, AcOH, THF 12 h, 81% (**26**), 77% (**28**), 84% (**30**); g) diglycolic anhydride, DMAP, pyridine, rt, 4 h, 51% (**5**), 65% (**6**), 74% (**12**).

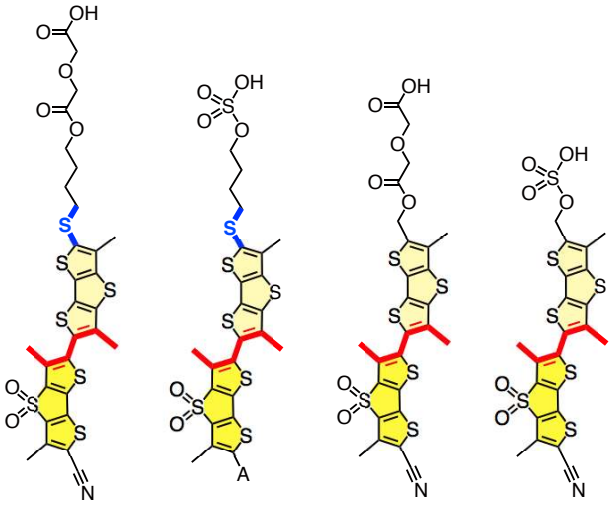

Figure 4. The second generation of twisted push-pull probes with turn-on sulfide donors, focusing on formyl and cyano acceptors and on pertinent controls.

Planarization in Single Crystals.

Amorphous powders of the original all-sulfur turn-on model probe **4** remained highly fluorescent (*Figs. 2*, *S11*). In single crystals of long, thin needles, the color was unchanged but fluorescence was completely quenched (*Fig. S11*). The X-ray structure revealed that in single crystals, model probe **4** is fully planarized (*Figs. 5*, *S12*). This planarization in single crystals is enforced by π-π stacking between the mechanophores. The distance of 3.8 Å between the neighboring aromatic planes was in agreement with this interpretation. The π-π stacking of the push-pull systems in single crystals is parallel. This finding suggested that packing forces overcompensate dipole repulsion (*Fig. 5a*).

Lateral contacts between DTTs in neighboring stacks are determined by chalcogen bonds (*Figs. 5b, c*).[14] One oxygen atom of the sulfone acceptors locates precisely in the focal point of the chalcogen bonds originating from the deep σ holes of the electron-deficient sulfur atoms of the DTT S,S-dioxides.

Planarization in DPPC Membranes.

Planarization of twisted push-pull probes with turn-on donors in lipid bilayer membranes was examined in large unilamellar vesicles (LUVs) composed of dipalmitoyl-*sn*-glycero-3-phosphocholine (DPPC). At 41 °C, DPPC LUVs show a phase transition from S_o to L_d membranes. Addition of the mechanophores to DPPC LUVs at 55 °C revealed their excitation and emission maxima in L_d membranes. Incubation times and concentrations were carefully adjusted to assure maximal partitioning of monomeric probes (*Fig. S1*). Linear concentration dependence of the fluorescence intensity was interpreted as indicative for monomeric probes (*Figs. 6*, *S2*). The appearance of saturation behavior at high concentration marked the onset of undesired side effects, including possible self-assembly of the probes in the L_d membranes or in solution. Non-linear regions in dose response curves were thus avoided for studies on ground-state planarization in S_o membranes.

With the original anchors with protonatable carboxylates, linear regions with monomeric probes were limited to low concentrations, usually only < 200 nM, which is < 0.3 mol% probe / lipid (*Fig. 6a*). The shortened anchors with permanent charges were introduced to prevent the self-assembly of the mechanophores. While more basic carboxylates could be partially protonated to facilitate their self-assembly with little charge repulsion, the less basic sulfonates could not in neutral buffer.[24] Consistent with these expectations, the spectroscopic properties of mechanophores with the new sulfonate anchors in lipid bilayer membranes were linear beyond 1 μM (*Fig. 6b*). Transient carboxylate protonation could also enable flip-flop of the probe to the inner leaflet of the bilayer by transient neutralization, which would be particularly problematic for the sensing of membrane potentials.[25]

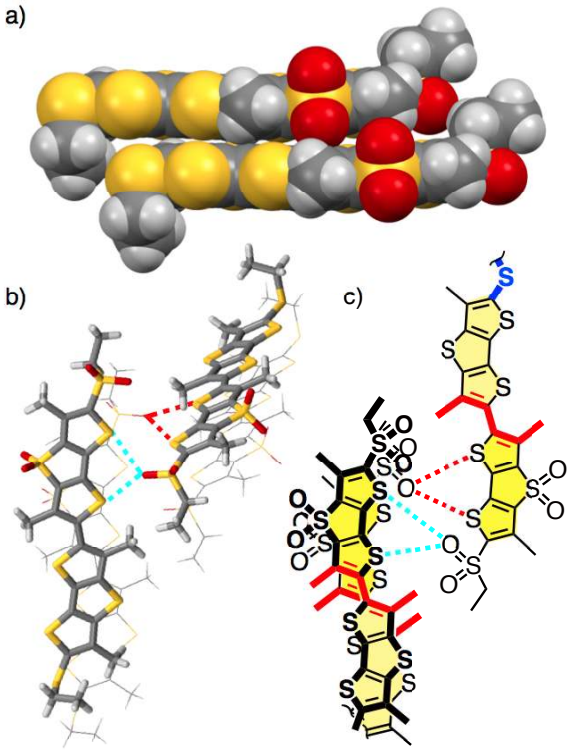

Figure 5. The crystal structure of planarized push-pull probe **4**. *a*) Side view of two monomers in space-filling presentation; *b*) Stick representation of two flippers from neighboring stacks; *c*) Chemdraw representation of the view in *b*). Intermolecular chalcogen bonds are highlighted in red and cyan.

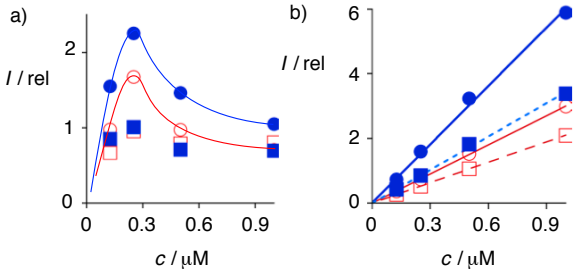

Figure 6. Concentration dependence of the emission of *a*) **12** and *b*) **7** in DPPC (●, ○) and DOPC LUVs (■, □) at 25 (●, ■) and 55 °C (○, □).

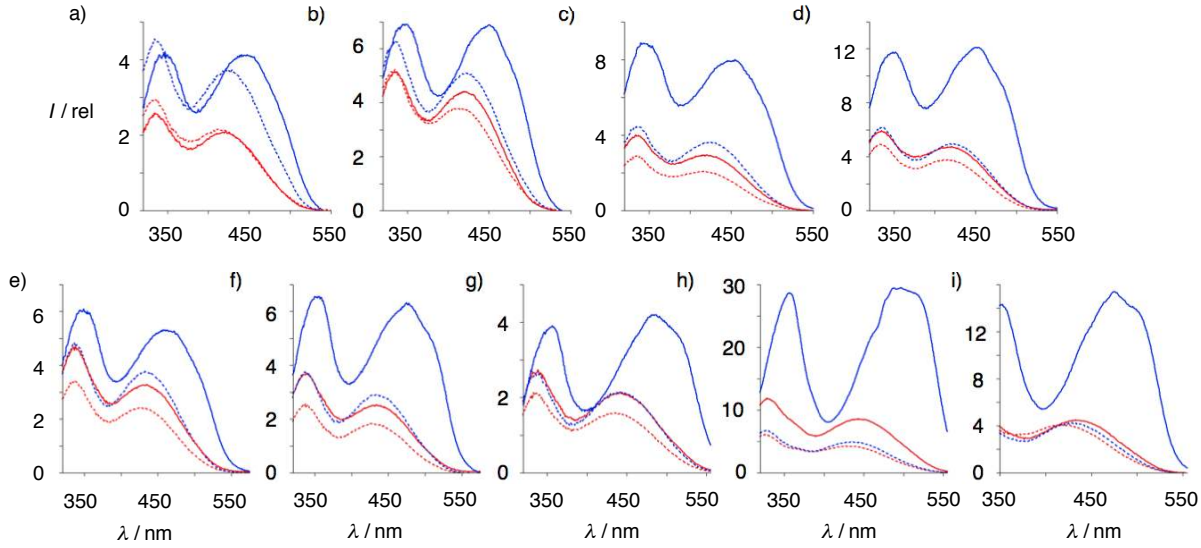

Figure 7. Excitation spectra in DPPC LUVs (solid) and DOPC LUVs (dotted) at 25 °C (blue) and 55 °C (red) for mechanophores *a*) **5**, *b*) **6**, *c*) **7**, *d*) **8**, *e*) **9**, *f*) **10**, *g*) **11**, *h*) **12** and *i*) **13** (λ_{em} at maximum).

After probe calibration in S_o membrane at 55 °C, the DPPC LUVs were cooled to 25 °C, and the spectroscopic response to the phase transition from liquid-disordered (L_d) to solid-ordered (S_o) membranes was recorded. To identify contributions from thermochromism, all experiments were repeated in dioleoyl-*sn*-glycero-3-phosphocholine (DOPC) LUVs, which are in L_d phase at both 25 °C and 55 °C.

In response to the transition from L_d to S_o DPPC membranes, the excitation maximum of all new probes **5–13** shifted to the red, without exception (*Table 1*, *Fig. 7*, solid). Red shifts $\Delta\lambda_{ex}$ consistently coincided with increases in fluorescence intensity ΔI. ΔI increased with $\Delta\lambda_{ex}$. The negligible shift found in emission upon phase transition of DPPC membrane (*Fig. S3*) or in excitation in DOPC upon cooling (*Fig. 7*, dashed) demonstrated that contributions from solvatochromism or thermochromism, respectively, are overall insignificant. These general trends suggested that the observed shifts in excitation originate from the ground-state planarization caused by the surrounding S_o membranes, thus identifying all new probes as operational mechanophores. Consistent trends with nine new probes provided much support for generality and robustness of the concept of fluorescent flippers.

The least convincing $\Delta\lambda_{ex}$ and ΔI were obtained with **5** and **6**, independent of the orientation of the macrodipole (*Table 1*, *Entries 1*, *2*; *Figs. 7a, b*). Shortening of the anionic tail without changes in the all-sulfur architecture of the mechanophore in **7** and **8** caused clear improvements (*Table 1*, *Entries 3*, *4*; *Figs. 7c, d*). Overlay of normalized spectra demonstrated that the orientation of the macrodipoles in the mechanophores in **5**–**8** is irrelevant (*Fig. 8a*).

Quantification of the often broad excitation maxima in S_o (but not L_d) membranes was not obvious (*Table 1*). The following format was selected: For clear maxima, this wavelength is indicated. For broad maxima, the midpoint of intercepts at 85% intensity is indicated as λ_{ex} together with, if appropriate, the bathochromic edge of bathochromic shoulders as λ_{ex}^S. Red shifts upon phase change are correspondingly referred to as $\Delta\lambda_{ex}$ and $\Delta\lambda_{ex}^S$. $\Delta\lambda_{ex}^S > \Delta\lambda_{ex}$ naturally always holds. Substitution of the sulfone in **7** with stronger formyl and cyano acceptors in **10** and **11** gradually shifted all excitation and emission maxima to the red in L_d DPPC membranes (*Table 1*, *Fig. 8b*, red). The same was true for sulfone and cyano acceptors in **5** and **9** with longer anchor without permanent charge (*Table 1*). Cooled down from L_d into S_o DPPC membranes, red shifts of the excitation maxima increased with push-pull strength from **5** / **7** to **9** / **10** and **11**, from $\Delta\lambda_{ex}$ = +25 nm to $\Delta\lambda_{ex}$ = +48 and $\Delta\lambda_{ex}^S$ = +79 nm (*Table 1*, *Fig. 8b*, blue). This was consistent with the stabilization of the planar conformer of the mechanophore by increasing strength of donors and acceptors.

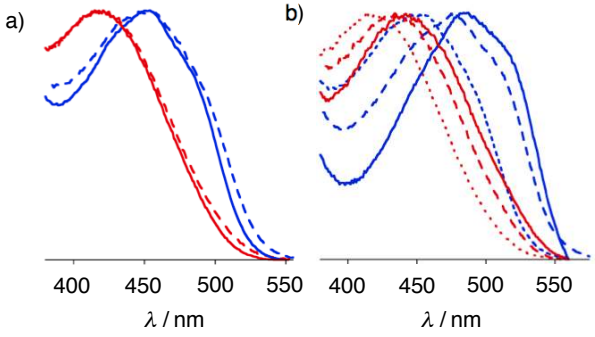

Figure 8. a) Macrodipole orientation: Normalized excitation spectra of **7** (dashed) and **8** (solid) in DPPC LUVs at 25 °C (blue) and 55 °C (red). b) Macrodipole strength: Normalized excitation spectra of **7** (dotted) **10** (dashed) and **11** (solid) in DPPC LUVs at 25 °C (blue) and 55 °C (red).

However, best results were obtained with **12** without turn-on sulfide donors, in which a cyano acceptor group replaces a formyl group of the original flipper architecture **3**. Upon cooling into S_o membranes, the excitation peak shifted to 501 nm, $\Delta\lambda_{ex}$ = +58 nm and ΔI = 3.5 were the largest in the series, and the bathochromic shoulder grew to full intensity up to (λ_{ex}^S = 522 nm, $\Delta\lambda_{ex}^S$ = +79 nm, *Table 1*, *Fig. 7h*).

Table 1. Spectroscopic properties of twisted push-pull probes in L_d and S_o DPPC LUVs.[a]

Cpd[b]	λ_{ex}^{55}/ nm[c]	λ_{ex}^{25}/ nm[d,e]	$\Delta\lambda_{ex}$/ nm[f,e]	ΔI_{ex}[g] (I_{ex}^{25})[h]
5	418	443	+25	2.0 (0.14)
6	419	446	+27	1.6 (0.23)
7	417	448	+31	2.7 (0.27)
8	416	448 (484)	+32 (+68)	2.6 (0.41)
9	430	459	+29	1.6 (0.18)
10	431	472 (510)	+41 (+79)	2.5 (0.21)
11	441	489 (520)	+48 (+79)	2.0 (0.14)
12	443	501 (522)	+58 (+79)	3.5 (1.00)
13	434	480 (503)	+46 (+69)	3.4 (0.52)

[a] See *Fig. 7* for original spectra. [b] Compounds, see *Figs. 3* and *4*. [c] Excitation maximum in DPPC LUVs at 55 °C. [d] Excitation maximum in DPPC LUVs at 25 °C. [e] For broad maxima, the midpoint of intercepts at 85% intensity is indicated and, if appropriate, the bathochromic edge of bathochromic shoulders in parentheses. Red shifts upon planarization are correspondingly referred to as $\Delta\lambda_{ex}$ and $\Delta\lambda_{ex}^{S}$ ($\Delta\lambda_{ex}^{S} > \Delta\lambda_{ex}$). [f] λ_{ex}^{25} minus λ_{ex}^{55} in DPPC LUVs. [g] Fluorescence intensity at the excitation maximum in DPPC LUVs at 25 °C divided by that in DPPC LUVs at 55 °C. [h] Fluorescence intensity in DPPC LUVs at 25 °C relative to **12**.

Shortening of the anionic anchor did not lead to further improvements: The bathochromic shoulder in minimalist flipper probe **13** lost in both intensity and shift (*Table 1*, *Fig. 7i*). Combination of the aldehyde acceptor and anionic anchors of matching length finally gave the best results for turn-on sulfide donors. In S_o DPPC, mechanophore **11** excelled with λ_{ex} = 489 nm, $\Delta\lambda_{ex}$ = +48 nm and a quite intense bathochromic shoulder at λ_{ex}^{S} = 520 nm, i.e., $\Delta\lambda_{ex}^{S}$ = +79 nm (*Table 1*, *Fig. 7g*). However, turn-on probes **11** with aldehyde acceptors (λ_{ex} = 489 nm, $\Delta\lambda_{ex}$ = +48 nm) remained inferior to conventional probes **12** with cyano acceptors (λ_{ex} = 501 nm, $\Delta\lambda_{ex}$ = +58 nm), not to speak of the original flipper **3** combining conventional "donors" with the same aldehyde acceptors (λ_{ex} = 515 nm, $\Delta\lambda_{ex}$ = +60 nm[15]).

Direct comparison of the turn-on sulfide donors with conventional "thenyl" esters was performed with cyano acceptors in **9**, **10** and **12** (*Fig. 4*). This comparison was meaningful from a functional point of view, to measure turn-on donors against the current best. For a structural point of view the two donors are less related, particularly considering likely contributions from intramolecular chalcogen bonding with thenyl esters (*Fig. 2*). Relevant donor comparison from structural point of view, *i.e.*, turn-on sulfides against the unstable ethers, has been reported.[17] In the present series, the couple **9** and **12** compares anchors of identical, removable charge. The couple **10** and **12** compares anchors of identical length. The clearly larger red shift of **10** (λ_{ex} = 472 nm, $\Delta\lambda_{ex}$ = +41 nm; λ_{ex}^{S} = 510 nm) compared to **9** (λ_{ex} = 459 nm, $\Delta\lambda_{ex}$ = +29 nm) in S_o membranes suggested that anchor length is more important than the nature of the charges (*Table 1*), at least at optimized high-dilution conditions (*Fig. 6*). Overall best results found with anchors of intermediate length compared to shorter (**13**) and longer ones were in agreement with this interpretation, highlighting the importance of precise probe positioning in the lipid bilayer membrane.

As in solution, the excitation of the optimized turn-on probe **10** (λ_{ex} = 431 nm) in L_d DPPC membranes was blue shifted compared to the conventional homolog **12** (λ_{ex} = 443 nm), whereas the emission of **10** (λ_{em} = 595 nm) was red shifted (**12**: λ_{em} = 585 nm, *Fig. 9*, *Table 1*). This enlarged Stokes shift was consistent with the concept of turn-on donors and promised increased mechanosensitivity upon planarization of the mechanophore in the ground state.[17] However, in S_o DPPC membranes, the maximum of turn-on probe **10** (λ_{ex} = 472 nm) clearly did not shift beyond that of **12** (λ_{ex} = 501 nm, *Fig. 9a*, *Tables 1* and *2*). The same was true for the bathochromic shoulder of **10** (λ_{ex}^{S} = 510 nm), which remained blue shifted and also clearly less intense than that of **12** (λ_{ex}^{S} = 522 nm, *Fig. 9a*, *Table 1*). This suggested that in S_o DPPC membranes, turn-on probes such as **10** are less planarized than conventional flippers **12**. Under these conditions, stabilization of the twisted conformer by the "turned off" sulfide acceptor appeared more effective than stabilization of the planar conformer by the "turned on" sulfide donor.

As with all mechanophores, emission of **10** and **12** did not much change upon L_d-S_o transition (*Fig. 9b*). As mentioned in the introduction, this general characteristic supports that twisted push-pull mechanophores act differently, i.e. by ground-state planarization, and are unrelated to established concepts such as molecular rotors or solvatochromism.[4][5]

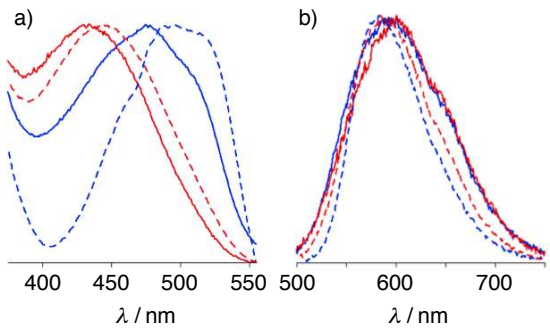

Figure 9. *a*) Excitation and *b*) emission spectra of **10** (solid) and **12** (dashed) in DPPC LUVs at 25 °C (blue) and 55 °C (red).

Planarization in Other Membranes.

The apparently incomplete planarization of turn-on flippers in S_o DPPC membranes suggested that in environments that are confining more or differently than the S_o phase of DPPC membranes, turn-on probe **10** but not conventional **12** could be further planarized. The apparently planar probes present in single crystals implied that complete planarization should be possible (*Fig. 5*). To elaborate on this hypothesis, saturated lipid bilayers of increasing thickness were considered first. Distearoyl-*sn*-glycero-3-phosphocholine (DSPC) membranes are formed by saturated lipids with 18 carbons in their alkyl tails, that is two more than in DPPC membranes. Compared to DPPC membranes with T_m = 41 °C, the transition from S_o to L_d DSPC membranes occurs at higher T_m = 55 °C.

As described for DPPC, turn-on probe **10** and the conventional homolog **12** were added to L_d DSPC and then cooled down into S_o DSPC membranes. The excitation spectra of the conventional **12** in S_o DSPC and DPPC were nearly superimposable (*Fig. 10b*). In clear contrast, the excitation spectrum of the turn-on probe **10** in S_o DSPC was much sharper than the one in S_o DPPC (*Fig. 10a*). The broad hypsochromic shoulder almost vanished, whereas the bathochromic shoulder increased. Estimated as half-width at 85% intensity, the formal λ_{ex} = 472 nm of turn-on probe **10** in S_o DPPC shifted to λ_{ex} = 488 nm in S_o DSPC LUVs (*Table 2*). This spectroscopic response was in agreement with increasing planarization of the twisted turn-on probe **10** with increasing thickness of S_o membranes.

The red shift of the twisted turn-on probe **10** in S_o DSPC membranes remained still $\Delta\lambda_{ex}$ = –10 nm inferior to that of the thickness insensitive conventional probe **12** (*Fig. 10*, *Table 2*, *Entry 2*). However, compared to the $\Delta\lambda_{ex}$ = –29 nm in S_o DPPC, the planarization of thickness sensitive turn-on **10** in S_o DSPC approaches that of the original flipper probe **12**.

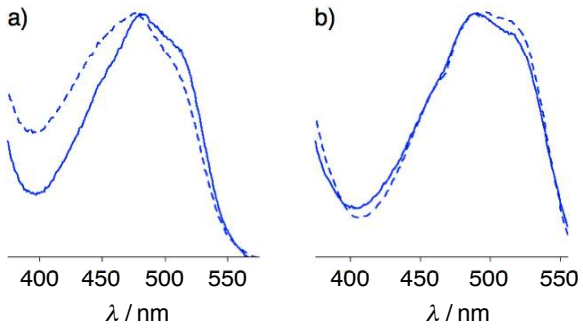

Figure 10. Excitation spectra of *a*) **10** and *b*) **12** in DPPC (dashed) and DSPC LUVs (solid) at 25 °C.

In egg yolk shingomyelin (SM) LUVs at 25 °C, the excitation maxima of both probes were blue shifted compared to S_o DPPC (*Fig. 11*, dashed, *Table 2*). Moreover, the difference in planarization $\Delta\lambda_{ex}$ = –36 nm between turn-on **10** and conventional **12** exceeded the $\Delta\lambda_{ex}$ = –29 nm in S_o DPPC (*Table 2*, *Entry 3 vs 1*). Quite remarkably, the presence of 33% cholesterol (CL) in SM membranes, that is the emergence of the liquid-ordered (L_o) phase, was simply not reported by conventional flippers **12** (*Fig. 11b*, solid, *Table 2, Entry 4 vs 3*). In contrast, the excitation maximum of turn-on probe **10** in SM/CL membranes shifted $\Delta\lambda_{ex}$ = +25 nm to the red. As in S_o DSPC membranes, the hypsochromic shoulder of the excitation maximum clearly decreased in SM/CL compared to SM membranes, and the bathochromic shoulder increased correspondingly (*Fig. 11a*). This suggested that planarization of turn-on probes **10** by the condensing effect of cholesterol in L_o phases is particularly effective. In L_o SM/CL membranes, the planarization of conventional probes **12** and turn-on probes **10** were almost equal ($\Delta\lambda_{ex}$ = –7 nm, *Fig. 11*, *Table 2, Entry 4*). Control experiments confirmed that the presence of cholesterol in DPPC/CL membranes (2:1) also red shifted of the excitation maxima of **10** in S_O DPPC membranes, but to a much less significant extent.

Table 2. Spectroscopic properties of turn-on and conventional flipper probes **10** and **12** in different hosts.[a]

Entry	Host[b]	λ_{ex}^{10}/ nm[c]	λ_{ex}^{12}/ nm[c]	$\Delta\lambda_{ex}$/ nm[d]
1	DPPC	472	501	–29
2	DSPC	488	498	–10
3	SM	456	492	–36
4	SM/CL	482	489	–7
5	α CD	-	-	-
6	β CD	391	392	–1
7	γ CD	456	464	–8
8	BSA	450	443	+7

[a] See *Fig. 4* for structures and *Figs. 10*, *11* and *13* for spectra. [b] DPPC: Dipalmitoyl-*sn*-glycero-3-phosphocholine LUVs at 25 °C; DSPC: Distearoyl-*sn*-glycero-3-phosphocholine LUVs at 25 °C; SM: Egg yolk sphingomyelin LUVs at 25 °C; SM/CL: SM/cholesterol 2:1 LUVs at 25 °C; CD: Cyclodextrin; BSA: Bovine serum albumin. [c] Excitation maximum. [d] λ_{ex}^{10} - λ_{ex}^{12}.

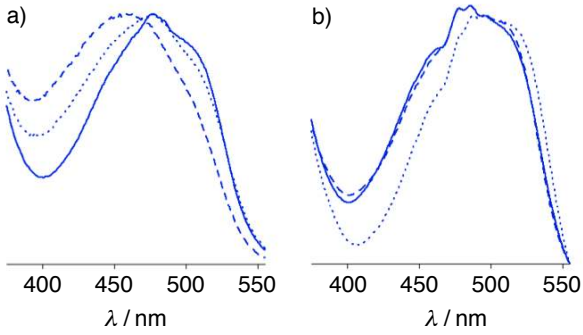

Figure 11. Excitation spectra of *a*) **10** and *b*) **12** in DPPC (dotted), SM (dashed) and SM/CL LUV (solid) at 25 °C.

In L_o SM/CL membranes, the fluorescence lifetime of turn-on probe **10** increased correspondingly to τ = 5.07 ± 0.05 ns. The blue shift of turn-on probe **10** in SM membranes coincided with a corresponding decrease to τ = 3.93 ± 0.03 ns, and the presence of cholesterol in L_d DOPC

membranes (τ = 2.06 ± 0.04 ns) increased lifetimes to τ = 3.57 ± 0.09 ns only, a value that is far below the long lifetimes reached in liquid-ordered membranes.

In summary, in S_o DPPC membranes, twisted flipper probes with turn-on donors are presumably less planarized than conventional mechanophores. Because of their already full planarization, conventional probes fail to report on further changes in highly-ordered membranes. In clear contrast, incomplete planarization of turn-on flippers in S_o DPPC membranes leaves room to respond to thicker S_o DSPC as well as to L_o SM/CL membranes with additional red shifts, i.e. further planarization.

Planarization in Macrocycles.

Cyclodextrins (CDs) are macrocyclic oligomers of α-1,4 glucopyranosides obtained from the enzymatic degradation of amylose.[26-33] Guest inclusion in their hydrophobic interior is used extensively to solubilize hydrophobic compounds in water. Moreover, molecular recognition within cyclodextrins has been applied to catalysis,[26][27] transport[28] and the self-assembly into higher-order architectures including multilayers on solid surfaces,[29] vesicles[30] as well as pseudorotaxanes and rotaxanes, particularly polyrotaxanes, in many variations.[31]

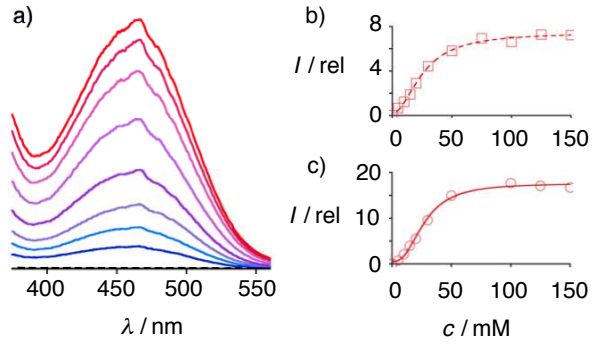

Figure 12. *a*) Increase in intensity in the excitation spectrum of turn-on flipper **10** with increasing concentration of γ CD in buffer. Dose response curve for γ CD with constant concentration of *b*) **10** and *c*) **12**.

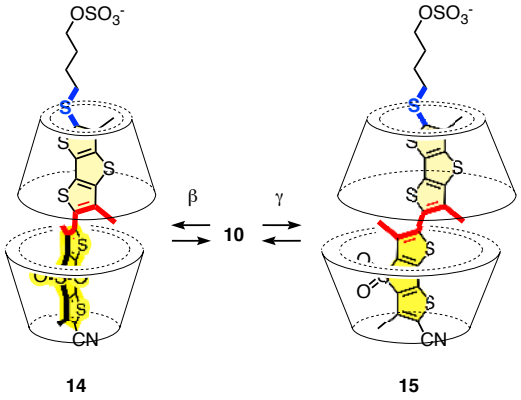

Figure 13. Notional structure of 2:1 pseudorotaxanes **14** and **15** formed by **10** with β and γ CD, respectively.

CDs are of interest as another type of confining environment of flippers. Inclusion of the flippers **10** and **12** in CDs would result in an increased fluorescence due to their sensitivity to the polarity of environment, typical for push-pull chromophores. Most common among CDs are α CD, a macrocycle composed of six glucose monomers with an internal diameter of 4.7 Å and a height of 7.9 Å, β CD with seven monomers and 6.0 Å internal diameter and γ CD with eight monomers and 7.5 Å internal diameter. In the presence of α CD, the fluorescence intensity of mechanophore **10** in Tris buffer at pH = 7.4 did not increase significantly (*Fig. S7*). With β CD, fluorescence intensities of turn-on mechanophore **10** in buffer increased dramatically with increasing CD concentration (*Fig. S8*). Dose response curves gave an EC_{50} = 7.8 ± 2.5 mM (*Fig. S8*). Comparable systems in the literature[31] and a Hill coefficient n = 1.8 ± 0.5 were consistent with the formation of 2:1 pseudorotaxane complexes such as **14** (*Fig. 13a*). The excitation maximum of complex **14** was at λ_{ex} = 391 nm, that is even more blue shifted than the λ_{ex} = 411 nm observed for turn-on flippers in solution (*Fig. 14a*, solid).

With γ CD, fluorescence intensities increased with a slightly less efficient EC_{50} = 25.9 ± 2.5 mM (*Figs. 12a, S9*). Hill coefficients of dose response curves remained with n = 2.0 ± 0.2 for **10** and n = 2.5 ± 0.3 for **12** and consistent with the formation of 2:1 pseudorotaxanes (*Figs. 12b, c, 13, S9*). The excitation maximum of turn-on mechanophore **10** in γ CD was at λ_{ex} = 456 nm (*Fig. 14a*, solid). The position of the maximum in γ CD was comparable to that of planarized probes in S_o membranes and $\Delta\lambda_{ex}$ = +65 nm red shifted compared to β CD. Compared to the conventional flipper **12**, the excitation maxima of the turn-on mechanophore **10** in γ CD was blue shifted by only $\Delta\lambda_{ex}$ = –8 nm (*Fig. 14a*, *Table 2, Entry 7*). This suggested that planarization of turn-on mechanophore **10** in γ CD is as effective as in SM/CL ($\Delta\lambda_{ex}$ = –7 nm) and DSPC LUVs ($\Delta\lambda_{ex}$ = –10 nm), and clearly better than DPPC membranes ($\Delta\lambda_{ex}$ = –29 nm, *Table 2*, *Fig. 14a*).

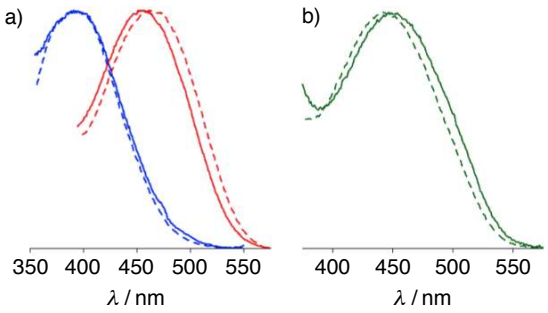

Figure 14. Excitation spectra of **10** (solid) and **12** (dashed) in *a*) β CD (blue), γ CD (red), and *b*) BSA.

Inspection of molecular models suggested that there is sufficient internal space available within β and γ CD to accommodate mechanophores without any tension. Overall, there are surprisingly few reports on spectroscopic changes that could be attributed to fluorophore twisting and untwisting with CD macrocycles.[31][32] Even planarization of carotenoids including astaxanthin within CDs failed because the β-ionone rings rather than the polyene chains were recognized exclusively.[27][33] Larger macrocycles like artificial[2] or biological β barrels[1] are needed to planarize carotenoids. The strong blue and red

shifts found for flipper mechanophores within β and γ CD, respectively, were thus quite interesting. Although there would be space for two flippers within γ CD, such dimerization appeared less likely considering Hill coefficients in support of 2:1 pseudorotaxanes **15** and a weaker fluorescence intensity expected for face-to-face dimerized flippers, which was not observed. The twisting and untwisting of flippers within CDs is thus likely to originate from interactions between the macrocycles in the expected pseudorotaxanes **14** and **15** (*Fig. 13*).

Planarization in Proteins.

Serum albumins are quite non-specific carrier proteins for hydrophobic ligands, including fatty acids and steroids.[34] In the presence of increasing concentrations of bovine serum albumin (BSA), fluorescence intensities of turn-on and conventional mechanophores **10** and **12** in water increased until saturation (*Fig. S10*). Measured for increasing protein concentration, the resulting dose response curves do not report on the number of mechanophores bound (crystal structures with up to seven fatty acids bound in various conformations to HSA have been reported[35]). However, they did reveal a most significant EC_{50} = 2.6 ± 1.1 μM for turn-on **10** and a more than two times weaker EC_{50} = 6.0 ± 1.4 μM for the conventional flipper **12** binding to BSA (*Fig. S10*). Their excitation maximum shifted to λ_{ex} = 450 nm and λ_{ex} = 443 nm, respectively (*Table 2*, *Fig. 14b*). This is thus the first example for excitation maxima of turn-on flippers **10** that exceed those of conventional probe **12**, i.e., $\Delta\lambda_{ex}$ = +7 nm, presumably indicating that in proteins, the turn-on flippers **10** are slightly more planarized than the original probe **12**.

Conclusions

The concept of turn-on donors aims to introduce substituents that act as acceptors in electron-rich aromatic systems and donors in electron-poor aromatic systems. In twisted push-pull mechanophores, turn-on donors are expected to support not only the deplanarization of the twisted "resting state" as acceptors, they should also stabilize the planar conformer in confined space as donors that strengthen the push-pull system. However, turn-on donors are attractive first to prevent the oxidative degradation in the twisted resting state and to easily functionalize both termini of the probe. Sulfides, characterized by positive σ_P and a negative σ_P^+, are the obvious choice to elaborate on turn-on donors. In S_o lipid bilayer membranes, nine new mechanophores with turn-on sulfides all show red shifts in excitation but not emission. This result is consistent with planarization of the new turn-on probes in the ground state, i.e., operational mechanophores. The mechanosensitivity of twisted push-pull probes with turn-on sulfide donors is best together with aldehyde acceptors and anionic anchors of matching, intermediate length, i.e., probe **11** (*Fig. 4*). Planarization in S_o DPPC membranes is independent of the orientation of the macrodipole of the push-pull probes, whereas increasing strength of the macrodipole not only shifts both excitation and emission maxima to the red but also increases mechanosensitivity. Length and nature of the anionic anchor are important for precise positioning of the probe within the membrane and to prevent probe aggregation by charge repulsion.

In S_o DPPC membranes, red shifts with turn-on mechanophores are smaller than with the original flipper probes. This weaker mechanosensitivity is consistent with incomplete planarization. This incomplete planarization indicated that, under these conditions, the stabilization of the deplanarized pull-pull conformers by sulfide acceptors is more effective than the stabilization of planarized push-pull conformers by turn-on sulfide donors. An apparently more reluctant planarization of turn-on probes promised sensitivity toward more confining environments. Indeed, turn-on mechanophores show particular sensitivity toward thicker S_o membranes (DSPC) as well as liquid-ordered membranes (SM/CL). In cyclodextrin pseudorotaxanes, shifts in excitation of the included mechanophores depend on the diameter and report, presumably, on interactions between the surrounding macrocycles. This switch is important because there is little precedence on mechanophore twisting in cyclodextrin pseudorotaxanes. Moreover, responsiveness to cyclodextrin-cyclodextrin interactions suggests that flipper mechanophores could be of interest not only as fluorescent membrane probes but also to sense intermolecular forces more generally, including tension in protein-protein interactions. Binding to proteins with confining hydrophobic pockets results in red shifts for turn-on probes that exceeds those of conventional mechanophores. This observation is important because it supports the implication from Stokes shifts that turn-on probes can maximize mechanosensitivity. Although overall consistent and meaningful, it is important to add that these interpretations are in part speculative and made with the only intention to rationalize results. They will naturally evolve in future with the emergence of new experimental data.

In summary, the results validate the concept of turn-on donors for operational mechanophores and identify specific characteristics of interest (e.g., stability in the twisted resting state, access to anchoring at both termini, mechanosensitivity toward differences at high confinement). Yet, in S_o DPPC membrane models, the original flipper probes **3**[15] and, with some reservations, also derivatives **12** and **13** with cyano acceptors remain superior with regard to absolute red shifts as well as absolute fluorescence intensity (*Fig. 2*). This conclusion is annoying because a) the origin of both effects is not understood, b) the probe tends to aggregate already at low concentrations and, most importantly, flippers with a "thenyl" ester decompose by an intriguing, possibly chalcogen-bond mediated, acid or base catalyzed fragmentation c) in cells and d) during modification of the terminal carboxylate.[36] However, these activated thenyl esters also account for the so far unique red shift and fluorescence intensity of the original probe **3**, presumably acting as long-distance donors to strengthen the push-pull system through 1,6 S-O chalcogen bonds (*Fig. 2*, ★★★).[36] The ultimate objective thus remains to find analogs of original **3** with a) stable, b) derivatizable and c) disaggregating anchors but preserved d) red shift, e) brightness and f) mechanosensitivity. Insights from this and coinciding studies[36] will contribute inspiration to tackle this important challenge, and although

less likely at this point, it cannot be excluded that the ultimate flipper probes will contain turn-on donors.

Experimental Section

See Supplementary Material.

Supplementary Material

Supporting information for this article is available on the WWW under http://dx.doi.org/10.1002/MS-number. CCDC-1505148 contains the supplementary crystallographic data for this work. These data can be obtained free of charge from The Cambridge Crystallographic Data Centre via www.ccdc.cam.ac.uk/data_request/cif.

Acknowledgements

We thank the NMR and the Sciences Mass Spectrometry (SMS) platforms for services, and the University of Geneva, the Swiss National Centre of Competence in Research (NCCR) Chemical Biology, the NCCR Molecular Systems Engineering and the Swiss NSF for financial support.

Author Contribution Statement

Q. V., N. S. and S. M. conceived this work; Q. V., A. R., L. G., N. S. and S. M. designed the experiments; Q. V., M. D. M., A. C. and L. G. conducted the experiments; Q. V., M. D. M., A. C., A. R., L. G., N. S. and S. M. discussed the results and commented on the manuscript, Q. V., N. S. and S. M. wrote the manuscript.

References

[1] a) A. P. Gamiz-Hernandez, I. N. Angelova, R. Send, D. Sundholm, V. R. I. Kaila, 'Protein-induced color shift of carotenoids in β-crustacyanin', *Angew. Chem. Int. Ed.* **2015**, *54*, 11564–11566; b) M. Helliwell, A. C. Regan, C. I. F. Watt, 'On the origin and variation of colors in lobster carapace', *Phys. Chem. Chem. Phys.* **2015**, *17*, 16723–16732.

[2] B. Baumeister, S. Matile, 'Rigid-rod β-barrels as lipocalin models: Probing confined space by carotenoid encapsulation', *Chem. Eur. J.* **2000**, *6*, 1739–1749.

[3] a) P. D. Kiser, M. Golczak, K. Palczewski, 'Chemistry of the retinoid (visual) cycle', *Chem. Rev.* **2014**, *114*, 194**–**232; b) M. Sheves, K. Nakanishi, B. Honig, 'Through-space electrostatic effects in electronic spectra. Experimental evidence for the external point-charge model of visual pigments', *J. Am. Chem. Soc.* **1979**, *101*, 7086–7088; c) T. Goto, T. Kondo, 'Structure and molecular stacking of anthocyanins - flower color variation', *Angew. Chem. Int. Ed.* **1991**, *30*, 17–33.

[4] a) T. Baumgart, G. Hunt, E. R. Farkas, W. W. Webb, G. W. Feigenson, 'Fluorescence probe partitioning between Lo/Ld phases in lipid membranes', *Biochim. Biophys. Acta* **2007**, *1768*, 2182–2194; b) I. A. Karpenko, M. Collot, L. Richert, C. Valencia, P. Villa, Y. Mély, M. Hibert, D. Bonnet, A. S. Klymchenko, 'Fluorogenic squaraine dimers with polarity-sensitive folding as bright far-red probes for background-free bioimaging', *J. Am. Chem. Soc.* **2015**, *137*, 405-412; c) I. López-Duarte, P. Chairatana, Y. Wu, J. Pérez-Moreno, P. M. Bennett, J. E. Reeve, I. Boczarow, W. Kaluza, N. A. Hosny, S. D. Stranks, R. J. Nicholas, K. Clays, M. K. Kuimova, H. L. Anderson, 'Thiophene-based dyes for probing membranes', *Org. Biomol. Chem.* **2015**, *13*, 3792–3802; d) L. A. Bagatolli, 'To see or not to see: lateral organization of biological membranes and fluorescence microscopy', *Biochim. Biophys. Acta* **2006**, *1758*, 1541–1556; e) E. Sezgin, F. Betul Can, F. Schneider, M. P. Clausen, S. Galiani, T. A. Stanly, D. Waithe, A. Colaco, A. Honigmann, D. Wüstner, F. Platt, C. Eggeling, 'A comparative study on fluorescent cholesterol analogs as versatile cellular reporters', *J. Lipid Res.* **2016**, *57*, 299–309.

[5] a) M. K. Kuimova, 'Mapping viscosity in cells using molecular rotors', *Phys. Chem. Chem. Phys.* **2012**, *14*, 12671–12686; b) X. Peng, Z. Yang, J. Wang, J. Fan, Y. He, F. Song, B. Wang, S. Sun, J. Qu, J. Qi, M. Yan, 'Fluorescence ratiometry and fluorescence lifetime imaging: using a single molecular sensor for dual mode imaging of cellular viscosity', *J. Am. Chem. Soc.* **2011**, *133*, 6626–6635; c) Z. Yang, Y. He, J.-H. Lee, N. Park, M. Suh, W.-S. Chae, J. Cao, X. Peng, H. Jung, C. Kang, J. S. Kim, 'A self-calibrating bipartite viscosity sensor for mitochondria', *J. Am. Chem. Soc.* **2013**, *135*, 9181–9185; d) M. Dakanali, T. H. Do, A. Horn, A. Chongchivivat, T. Jarusreni, D. Lichlyter, G. Guizzunti, M. A. Haidekker, E. A. Theodorakis, 'Self-calibrating viscosity probes: design and subcellular localization', *Bioorg. Med. Chem.* **2012**, *20*, 4443–4450; e) T. Muraoka, T. Endo, K. V. Tabata, H. Noji, S. Nagatoishi, K. Tsumoto, R. Li, K. Kinbara, Reversible ion transportation switch by a ligand-gated synthetic supramolecular ion channel, *J. Am. Chem. Soc.* **2014**, *136*, 15584-15595; f) Y. Niko, P. Didier, Y. Mely, G. Konishi, A. S. Klymchenko, Bright and photostable push-pull pyrene dye visualizes lipid order variation between plasma and intracellular membranes', *Sci. Rep.* **2016**, *6*, 18870.

[6] a) C. R. Woodford, E. P. Frady, E. P.; Smith, R. S.; Morey, B.; Canzi, G.; Palida S. F.; Araneda R. C.; Kristan W. B.; Kubiak, C. P.; Miller, E. W.; Tsien, R. Y. 'Improved PeT molecules for optically sensing voltage in neurons', *J. Am. Chem. Soc.* **2015**, *137*, 1817–1824; b) W. Miller, J. Y. Lin, E. P. Frady, P. A. Steinbach, W. B. Kristan Jr, R. Y. Tsien, 'Optically monitoring voltage in neurons by photo-induced electron transfer through molecular wires', *Proc. Natl. Acad. Sci. USA* **2012**, *109*, 2114–2119; c) P. Yan, A. Xie, M. Wei and L. M. Loew, 'Amino(oligo)thiophene-based environmentally sensitive biomembrane chromophores', *J. Org. Chem.*, 2008, **73**, 6587–6594; d) N. Sakai, S. Matile, 'Recognition of polarized lipid bilayers by p-oligophenyl ion channels: from push-pull rods to push-pull barrels', *J. Am. Chem. Soc.* **2002**, *124*, 1184–1185; e) J.-Y. Winum, S. Matile, 'Rigid push-pull oligo(*p*-phenylene) rods: Depolarization of bilayer membranes with negative membrane potential', *J. Am. Chem. Soc.* **1999**, *121*, 7961–7962.

[7] N. Sakai, D. Gerard, S. Matile, 'Electrostatics of cell membrane recognition: Structure and activity of neutral and cationic rigid push-pull rods in isoelectric, anionic, and polarized lipid bilayer membranes', *J. Am. Chem. Soc.* **2001**, *123*, 2517–2524.

[8] A. Diz-Munoz, D. A. Fletcher, O. D. Weiner, 'Use the force: membrane tension as an organizer of cell shape and motility', *Trends Cell Biol.* **2013**, *23*, 47–53.

[9] a) M. M. Caruso, D. A. Davis, Q. Shen, S. A. Odom, N. R. Sottos, S. R. White, J. S. Moore, 'Mechanically-induced chemical changes in polymeric materials', *Chem. Rev.* **2009**, *109*, 5755–5798; b) R. Groote, R. T. M. Jakobs, R. P. Sijbesma, 'Mechanocatalysis: Forcing latent catalysts into action', *Polym. Chem.* **2013**, *4*, 4846–4859; c) J. Kim**,** T. M. Swager, **'**Control of conformational and interpolymer effects in conjugated polymers', *Nature* **2001**, *411*, 1030–1034; d) R. H. Pawle, T. E. Haas, P. Müller, S. W. Thomas III, 'Twisting and piezochromism of phenylene-ethynylenes with aromatic interactions between side chains and main chains', *Chem. Sci.* **2014**, *5*, 4184–4188; e) H. Dube, M. R. Ams and J. Rebek Jr, 'Supramolecular control of fluorescence through reversible encapsulation', *J. Am. Chem. Soc.* **2010**, *132*, 9984–9985; f) F. Chen, J. Zhang, X. Wan, 'Design and synthesis of piezochromic materials based on push–pull chromophores: A mechanistic perspective', *Chem. Eur. J.* **2012**, *18*, 4558-4567; g) Y. Ooyama, Y. Harima, 'Molecular design of

mechanofluorochromic dyes and their solid-state fluorescence properties', *J. Mater. Chem.* **2011**, *21*, 8372–8380; h) B. R. Crenshaw, C. Weder, 'Deformation-induced color changes in melt-processed photoluminescent polymer blends', *Chem. Mater.* **2003**, *15*, 4717–4724; i) F. Ciardelli, G. Ruggeri, A. Pucci, 'Dye-containing polymers: methods for preparation of mechanochromic materials', *Chem. Soc. Rev.* **2013**, *42*, 857-870; j) Z. Zhang, Y.-S. Wu, K.-C. Tang, C.-L. Chen, J.-W. Ho, J. Su, H. Tian, P.-T. Chou, Excited-state conformational/electronic responses of saddle-shaped *N*,*N*′-disubstituted-dihydrodibenzo[*a*,*c*]phenazines: Wide-tuning emission from red to deep blue and white light combination', *J. Am. Chem. Soc.* **2015**, 137, 8509–8520; k) S. Wiedbrauk, B. Maerz, E. Samoylova, A. Reiner, F. Trommer, P. Mayer, W. Zinth, H. Dube, 'Twisted hemithioindigo photoswitches: solvent polarity determines the type of light-induced rotations', *J. Am. Chem. Soc.* **2016**, *138*, 12219–12227.

[10] a) C. Reichardt, 'Solvatochromic dyes as solvent polarity indicators', *Chem. Rev.* **1994**, *94*, 2319–2358; b) B. Maerz, S. Wiedbrauk, S. Oesterling, E. Samoylova, A. Nenov, P. Mayer, R. de Vivie-Riedle, W. Zinth, H. Dube, Making fast photoswitches faster - Using Hammett analysis to understand the limit of donor–acceptor approaches for faster hemithioindigo photoswitches', *Chem. Eur. J.* **2014**, *20*, 13984-13992; c) G. Sotgiu, M. Galeotti, C. Samorí, A. Bongini, A. Mazzanti, 'Push–pull amino succinimidyl ester thiophene-based fluorescent dyes: Synthesis and optical characterization', *Chem. Eur. J.* **2011**, 17, 7947–7952; d) K. Fujisawa, M. Humbert-Droz, R. Letrun, E. Vauthey, T. A. Wesolowski, N. Sakai, S. Matile, 'Ion pair–π interactions', *J. Am. Chem. Soc.* **2015**, *13*, 11047–11056; e) F. Effenberger, F. Würthner, '5-Dimethylamino-5′-nitro-2, 2′-bithiophene - a new dye with pronounced positive solvatochromism', *Angew. Chem. Int. Ed.* **1993**, *32*, 719–721; f) E. E. Nesterov, J. Skoch, B. T. Hyman, W. E. Klunk, B. J. Bacskai, T. M. Swager, 'In vivo optical imaging of amyloid aggregates in brain: design of fluorescent markers', *Angew. Chem. Int. Ed.* **2005**, *44*, 5452–5456; g) Z. Lu, N. Liu, S. J. Lord, S. D. Bunge, W. E. Moerner, R. J. Twieg, 'Bright, red single-molecule emitters: Synthesis and properties of environmentally sensitive dicyanomethylenedihydrofuran (DCDHF) fluorophores with bisaromatic conjugation', *Chem. Mater.* **2009**, *21*, 797–810; h) S. Sasaki, Y. Niko, A. S. Klymchenko, G. Konishi, 'Design of donor–acceptor geometry for tuning excited-state polarization: fluorescence solvatochromism of push–pull biphenyls with various torsional restrictions on their aryl–aryl bonds', *Tetrahedron* **2014**, *70*, 7551–7559; i) S. Richert, S. Mosquera Vazquez, M. Grzybowski, D. T. Gryko, A. Kyrychenko, E. Vauthey, 'Excited-state dynamics of an environment-sensitive push-pull diketopyrrolopyrrole: Major differences between the bulk solution phase and the dodecane/water interface', *J. Phys. Chem. B* **2014**, *118*, 9952–9963.

[11] A. Fin, A. Vargas-Jentzsch, N. Sakai, S. Matile, 'Oligothiophene amphiphiles as planarizable and polarizable fluorescent membrane probes', *Angew. Chem. Int. Ed.* **2012**, *51*, 12736–12739.

[12] D. Alonso Doval, M. Dal Molin, S. Ward, A. Fin, N. Sakai, S. Matile, 'Planarizable push-pull oligothiophenes: In search of the perfect twist', *Chem. Sci.* **2014**, *5*, 2819–2825.

[13] a) A. Mishra, C. Ma, P. Bäuerle, 'Functional oligothiophenes: Molecular design for multidimensional nanoarchitectures and their applications', *Chem. Rev.* **2009**, *109*, 1141–1276; b) J. Roncali, P. Blanchard, P. Frère, '3,4-Ethylenedioxythiophene (EDOT) as a versatile building block for advanced functional π-conjugated systems', *J. Mater. Chem.* **2005**, *15*, 1589–1610; c) I. Osaka, R. D. McCullough, 'Advances in molecular design and synthesis of regioregular polythiophenes', *Acc. Chem. Res.* **2008**, *41*, 1202–1214; d) Y. Ie, A. Han, T. Otsubo, Y. Aso, 'Completely encapsulated oligothiophenes up to 12-mer', *Chem. Commun.* **2009**, *21*, 3020–3022; e) T. Klingstedt, H. Shirani, K. O. A. Åslund, N. J. Cairns, C. J. Sigurdson, M. Goedert, K. P. R. Nilsson, 'The structural basis for optimal performance of oligothiophene-based fluorescent amyloid ligands: conformational flexibility is essential for spectral assignment of a diversity of protein aggregates', *Chem. Eur. J.* **2013**, *19*, 10179–10192; f) H.-A. Ho, A. Najari, M. Leclerc, 'Optical detection of DNA and proteins with cationic polythiophenes', *Acc. Chem. Res.* **2008**, *41*, 168–178.

[14] a) B. R. Beno, K.-S. Yeung, M. D. Bartberger, L. D. Pennington, N. A. Meanwell, 'A survey of the role of noncovalent sulfur interactions in drug design', *J. Med. Chem.* **2015**, *58*, 4383–4438; b) A. Bauzà, T. J. Mooibroek, A. Frontera, 'The bright future of unconventional σ/π-hole interactions', *ChemPhysChem* **2015**, *16*, 2496–2517; c) J. Fanfrlík, A. Prada, Z. Padelkova, A. Pecina, J. Machacek, M. Lepsik, J. Holub, A. Ruzicka, D. Hnyk, P. Hobza, 'The dominant role of chalcogen bonding in the crystal packing of 2D/3D aromatics', *Angew. Chem. Int. Ed.* **2014**, *53*, 10139–10142; d) A. Kremer, A. Fermi, N. Biot, J. Wouters, D. Bonifazi, 'Supramolecular wiring of benzo-1,3-chalcogenazoles through programmed chalcogen bonding interactions', *Chem. Eur. J.* **2016**, *22*, 5665–5675; e) G. E. Garrett, G. L. Gibson, R. N. Straus, D. S. Seferos, M. S. Taylor, 'Chalcogen bonding in solution: interactions of benzotelluradiazoles with anionic and uncharged Lewis bases', *J. Am. Chem. Soc.* **2015**, *137*, 4126-4133; f) S. Benz, M. Macchione, Q. Verolet, J. Mareda, N. Sakai, S. Matile, 'Anion transport with chalcogen bonds', *J. Am. Chem. Soc.* **2016**, *138*, 9093–9096.

[15] M. Dal Molin, Q. Verolet, A. Colom, R. Letrun, E. Derivery, M. Gonzalez-Gaitan, E. Vauthey, A. Roux, N. Sakai, S. Matile, 'Fluorescent flippers for mechanosensitive membrane probes', *J. Am. Chem. Soc.*, **2015**, *137*, 568–571.

[16] a) M. E. Cinar, T. Ozturk, 'Thienothiophenes, dithienothiophenes, and thienoacenes: syntheses, oligomers, polymers, and properties', *Chem. Rev.* **2015**, *115*, 3036–3140; b) G. Barbarella, F. Di Maria, 'Supramolecular oligothiophene microfibers spontaneously assembled on surfaces or coassembled with proteins inside live cells', *Acc. Chem. Res.* **2015**, *48*, 2230–2241; c) G. Barbarella, 'Oligothiophene isothiocyanates as fluorescent markers', *Chem. Eur. J.* **2002**, *8*, 5072–5077; d) F. De Jong, M. J. Janssen, 'Synthesis, oxidation, and electronic spectra of four dithienothiophenes', *J. Org. Chem.* **1971**, *36*, 1645–1648; e) X. He, J. Borau-Garcia, A. Y. Y. Woo, S. Trudel, T. Baumgartner, 'Dithieno[3,2-c:2',3'-e]-2,7-diketophosphepin: a unique building block for multifunctional π-conjugated materials', *J. Am. Chem. Soc.* **2013**, *135*, 1137–1147.

[17] Q. Verolet, A. Rosspeintner, S. Soleimanpour, N. Sakai, E. Vauthey, S. Matile, 'Turn-on sulfide π donors: An ultrafast push for twisted mechanophores', *J. Am. Chem. Soc.* **2015**, *137*, 15644–15647.

[18] F. Bernardi, A. Mangini, N. D. Epiotis, J. R. Larson, S. Shaik, 'The π-donating ability of heteroatoms', *J. Am. Chem. Soc.* **1977**, *99*, 7465–7470.

[19] a) L. P. Hammett, 'The effect of structure upon the reactions of organic compounds. Benzene derivatives', *J. Am. Chem. Soc.* **1937**, *59*, 96–103; b) C. Hansch, A. Leo, R. W. Taft, 'A survey of Hammett substituent constants and resonance and field parameters', *Chem. Rev.* **1991**, *91*, 420–427.

[20] D. Seebach, 'Methods of reactivity umpolung', *Angew. Chem. Int. Ed.* **1979**, *18*, 239-336.

[21] N. Takeda, N. Tokitoh, R. Okazaki, Synthesis, structure, and reactions of the first rotational isomers of stable thiobenzaldehydes, 2,4,6-tris[bis(trimethylsilyl)methyl]thiobenzaldehydes', *Chem. Eur. J.* **1997**, *3* , 62–69.

[22] F. N. Miros, S. Matile, 'Core-substituted naphthalenediimides: LUMO levels revisited, in Comparison with perylenediimides with sulfur redox switches in the core', *ChemistryOpen* **2016**, *5*, 219–226.

[23] See SI.

[24] N. Chuard, K. Fujisawa, P. Morelli, J. Saarbach, N. Winssinger, P. Metrangolo, G. Resnati, N. Sakai, S. Matile, 'Activation of cell-penetrating peptides with

ionpair-π interactions and fluorophiles', *J. Am. Chem. Soc.* **2016**, *138*, 9093–9096.

[25] V. Gorteau, G. Bollot, J. Mareda, S. Matile, 'Rigid-rod anion–π slides for multiion hopping across lipid bilayers', *Org. Biomol. Chem.* **2007**, *5*, 3000–3012.

[26] R. Breslow, S. D. Dong, Biomimetic reactions catalyzed by cyclodextrins and their derivatives', *Chem. Rev.* **1998**, *98*, 1997–2011.

[27] R. R. French, P. Holzer, M. G. Leuenberger, W.-D. Woggon, 'A supramolecular enzyme mimic that catalyzes the 15,15' double bond scission of β,β-carotene', *Angew. Chem. Int. Ed.* **2000**, *39*, 1267–1269.

[28] a) N. Sakai, S. Matile, 'Synthetic ion channels', *Langmuir* **2013**, *29*, 9031–9040; b) I. Tabushi, Y. Kuroda, K. Yokota, 'A,B,D,F-tetrasubstituted β-cyclodextrin as artificial channel compound', *Tetrahedron Lett.* **1982**, *23*, 4601–4604.

[29] M. J. W. Ludden, D. N. Reinhoudt, J. Huskens, 'Molecular printboards: versatile platforms for the creation and positioning of supramolecular assemblies and materials', *Chem. Soc. Rev.* **2006**, *35*, 1122–1134.

[30] F. Schibilla, L. Stegemann, C. A. Strassert, F. Rizzo, B. J. Ravoo, 'Fluorescence quenching in β-cyclodextrin vesicles: membrane confinement and host–guest interactions', *Photochem. Photobiol. Sci.* **2016**, *15*, 235–243.

[31] a) M. J. Frampton, H. L. Anderson, 'Insulated molecular wires', *Angew. Chem. Int. Ed.* **2007**, *46*, 1028–1064; b) A. Harada, A. Hashidzume, H. Yamaguchi, Y. Takashima, 'Polymeric Rotaxanes', *Chem. Rev.* **2009**, *109*, 5974–6023.

[32] S. Kasiouli, F. Di Stasio, S. O. McDonnell, C. P. Constantinides, H. L. Anderson, F. Cacialli, S. C. Hayes, 'Resonance Raman investigation of β-cyclodextrin-encapsulated π-conjugated polymers', *J. Phys. Chem. B* **2013**, *117*, 5737–5747.

[33] C. Yuan, Z. Jin, X. Xu, 'Inclusion complex of astaxanthin with hydroxypropyl-β-cyclodextrin: UV, FTIR, 1H NMR and molecular modeling studies', *Carbohyd. Polym.* **2012**, *89*, 492–496.

[34] A. Varshney, P. Sen, E. Ahmad, M. Rehan, N. Subbarao, R. H. Khan, 'Ligand binding strategies of human serum albumin: how can the cargo be utilized?', *Chirality* **2010**, *22*, 77–87.

[35] I. Petitpas, T. Grüne, A. A. Bhattacharya, S. Curry, 'Crystal structures of human serum albumin complexed with monounsaturated and polyunsaturated fatty acids', *J. Mol. Biol.* **2001**, *314*, 955–960.

[36] S. Soleimanpour, A. Colom, E. Derivery, M. Gonzalez-Gaitan, A. Roux, N. Sakai, S. Matile, 'Headgroup engineering in mechanosensitive membrane probes', unpublished.

Entry for the Table of Contents

((Insert TOC Graphic here; max. width: 17.5 cm; max. height: 7.0 cm))